Thermochimica Acta 727 (2023) 179575

Contents lists available at ScienceDirect

Thermochimica Acta

journal homepage: www.elsevier.com/locate/tca

The use of isothermal calorimetry to measure corrosion rates of metals in contact with preservative-treated wood

Samuel L. Zelinka *, Samuel V. Glass, Eleanor Q.D. Lazarcik

ARTICLE INFO

Keywords:
Preservative treated wood
Hot-dip galvanized steel
Corrosion
Isothermal microcalorimetry
Moisture

ABSTRACT

The purpose of this paper is to examine whether isothermal microcalorimetry can be used to determine the corrosion rates of metals embedded in wood. Metal fasteners were driven into dowels of wood treated with alkaline copper quaternary, a common wood preservative that increases the corrosiveness of wood. The dowels were stored in a nearly 100% relative humidity environment at 27°C for one year; throughout the exposure period, dowels were removed and the thermal power generated by the sample was measured in an isothermal calorimeter. Measurements over the 1-year exposure showed that the thermal power depended upon the wood moisture content and ranged from 0 to 200 μW. The heat, determined by integrating thermal power over time, was higher than expected compared with the total amount of mass lost due to corrosion at the end of the experiment. Despite this, the technique shows promise as a method to determine how changes in wood moisture content affect the corrosion rates of metals in contact with preservative treated wood.

1. Introduction

Typical corrosion testing falls into three major categories: exposure testing, accelerated aging tests, and electrochemical tests. Exposure tests, where metals are placed into the environment of interest and removed after they have corroded, yield the best prediction of corrosion rates of materials under actual service conditions. However, these tests require a long exposure duration. For example, some corrosion tests of metals in treated wood have been run for 19 years [1]. Because these long exposure times are often impractical, accelerated aging or electrochemical tests are often used instead.

Accelerated aging tests are commonly used to screen different coatings on metals. Accelerated aging tests can sometimes be used if the corrosion mechanism is well understood and the accelerating factors are appropriate. For example, one common accelerated aging test uses a "salt-spray" test where metals are exposed to cyclic conditions of salinated water, humidity, and a dry environment [2]; this method has been shown to correlate with in-service exposure lifetimes for materials undergoing uniform corrosion [3,4]. Similar test methods may often add UV or IR exposure as additional accelerating factors [5]. However, accelerated aging tests often only accelerate environmental conditions and often cannot account for biologically influenced corrosion. As a result, these methods often cannot be correlated to in-service corrosion rates [6–9]. This is especially true for complex environmental conditions, such as fasteners embedded in wood, or rebar embedded in concrete.

Finally, electrochemical tests can be performed in aqueous environments using a potentiostat. By sweeping across electric potentials the activation energy is changed and the resulting electrical current can be used to determine the corrosion rate [10]. Electrochemical tests can measure very low corrosion rates (less than 1 μm yr^{-1}) in just a few minutes. However, these measurements work best in aqueous environments.

All three of these types of corrosion measurements have been used to measure the corrosion of metals in contact with wood which has been studied for over 100 years [11,12]. Fasteners embedded in wood are subject to corrosion from the moisture and organic acids within the wood structure along with any treatment chemicals added to the wood [13–16]. The complex interaction of moisture and treatment chemicals make it difficult to accelerate by changing the environmental conditions. However, there are two standardized test for measuring the corrosion rates of metals in contact with treated wood that use challenging environmental conditions to accelerate the corrosion rate [17–19]. Electrochemical tests in solid wood are uniquely challenging because wood is an ionic conductor [20–22]. To avoid these inherent difficulties, Zelinka et al. [23,24] developed an electrochemical test where fasteners were placed in a water-extract of treated wood. They demonstrated that this method had good correlation to long-term exposure tests in moist wood. However, only limited data on the wood moisture content dependence of the corrosion rate can be gathered from these techniques [25–27].

The corrosion of metals in wood has been shown to be a strong

* Corresponding author.
E-mail address: samuel.l.zelinka@usda.gov (S.L. Zelinka).

https://doi.org/10.1016/j.tca.2023.179575
Received 25 May 2023; Received in revised form 11 July 2023; Accepted 17 July 2023
Available online 17 July 2023
0040-6031/Published by Elsevier B.V.

function of moisture content; below 15-18% wood moisture content (MC), embedded metals do not corrode [15,16]. The first data on the moisture dependence of corrosion of metals was produced by Short, Dennis, and Zou [25,26]. These researchers placed metal sheets between pieces of wood at a known moisture content and used the polarization resistance technique to measure corrosion rates. They found that there was no measurable corrosion at 15% MC and that the corrosion rate increased sharply from 20% MC to 30% MC before reaching a plateau. Later, Zelinka, et al. [27] tried to replicate these experiments. While they also found that corrosion essentially stopped below 18% MC, there was too much variability in the measurements to draw conclusions about how moisture content affected the corrosion rate. Furthermore, resistance of the wood increases as the wood moisture content deceases making these measurements highly uncertain at low moisture contents. Since the wood moisture content plays such a critical role in the corrosion rate, a method to measure corrosion at a given wood moisture content would be extremely useful.

In most environments, corrosion rates decrease with time (t) because metals form a passive layer that reduces the corrosion rate and corrosion exhibits a t^n behavior (where n is between 0.5 and 1) [28,29]. However, the limited corrosion data that exist on the corrosion of metals in wood suggests that the corrosion rate remains constant with time (i.e. n=1). More plainly speaking, the n=1 behavior indicates that no protective passive layer is formed. Baker found that the total amount of corrosion increased linearly with time (i.e. constant corrosion rate) for fasteners embedded in wood between 1 and 19 years but did not measure any data during the first year [1]. Zelinka measured gravimetric corrosion rates between 4 and 48 weeks and found a slight decrease in the corrosion rate at longer times but did not have enough replicates for a statistical comparison and there was a high amount of uncertainty and variation in the data at early time points [30]. The fact that wood appears to exhibit a constant corrosion rate with time has been used to develop predictive models of both the cumulative amount of corrosion that will occur in various climates and the loss of capacity of the wood-metal joint [31,32]. However, since this kinetic behavior is so unusual, it should be confirmed by additional experimental evidence.

In this paper we attempt to use isothermal calorimetry to monitor the corrosion rate *in-situ* during a one-year exposure test. In isothermal calorimetry, a specimen is placed in a constant temperature environment and the thermal power of the reaction is measured. The technique has been used to study chemical and biological systems since the 1700s [33,34]. It is frequently used to measure ligand binding reactions, curing of concrete, degradation of chemical compounds, and biological reactions [35–37].

However, few studies have used isothermal microcalorimetry to measure corrosion. In many cases, the measurements were used to compare the relative effectiveness of a treatment or material. For example, Telegdi et al. [38,39] used the technique to measure the effectiveness of self-assembled monolayer coatings by comparing the total enthalpy between coated and uncoated samples after the first 20 minutes of exposure to a corrosive solution. Likewise, Tomantschger et al. [40] examined carbon corrosion in various fuel cell electrode configurations for up to 1500 hours. Since only relative changes were examined, the corrosion rates were reported in μW rather than g yr^{-1} or μm yr^{-1}. Even fewer studies have used microcalorimetry to determine physical corrosion rates. Chin et al. [41] measured the thermal power released by liquid propellent in a metal container to obtain kinetic parameters to build a corrosion model. They reported both corrosion rates in mm yr^{-1} and μW cm^{-2}; however, it is unclear whether they used tabulated enthalpies or an empirical correlation to convert these values.

Only a few studies have compared corrosion rates measured in the isothermal calorimeter directly to a complimentary technique. These studies examined the corrosion of magnesium in saline solutions and the hydrogen gas evolved from the corrosion reaction was measured simultaneously [42,43]. Since the amount of hydrogen gas produced is directly proportional to the mass of Mg that corroded, it was possible to instantaneously measure the corrosion reaction rate using both calorimetry and stoichiometry. Through this double measurement, they found the experimental reaction enthalpy (375 ±15 kJ mol^{-1}) was close to literature values of 350 kJ mol^{-1}. In summary, isothermal microcalorimetry shows promise for measuring the instantaneous corrosion rate of many materials although only limited work has been done where corrosion rates have been confirmed with a secondary technique.

This paper evaluates whether isothermal microcalorimetry can be used to measure the corrosion of metals embedded in wood on one type of treated wood. While the absolute value of the measured corrosion rates will depend upon the preservative formulation used, these measurements are intended to be a proof of concept of the experimental method. Ultimately, we envision that isothermal microcalorimetry could be an effective rapid test method for measuring the corrosion rates of metals in wood because it yields the instantaneous corrosion rate during typical exposure conditions in the non-aqueous electrolyte of wood. As such, it combines the rapid results of an accelerated exposure test with the benefit of the measurement being made in the exact environment of interest. Furthermore, the method is well suited for probing the relationship between the corrosion rate and wood moisture content at low moisture contents and since it is a non-destructive measurement of corrosion, it could be used to monitor long-term corrosion tests to confirm whether the corrosion kinetics remain constant with time.

2. Materials and methods

2.1. Materials

The wood samples were made from eastern white pine (*Pinus strobus*) dowel stock with a dimeter of 16 mm. Dowels were cut into 45 mm segments. The dowels contained both heartwood and sapwood. In general, sapwood absorbs more preservative treatment than heartwood and the presence of heartwood may have affected the distribution of preservative treatment within the dowels. The dowels were treated with a commonly used commercial wood preservative, ammoniacal copper quaternary type D (ACQ-D) made with a carbonate salt formulation, as described in the American Wood Protection Association product standard P-5 [44]. The composition of ACQ-D in the P-5 standard consists of 67% copper as copper oxide and 33% dim didecyldimethylammonium carbonate. The samples were treated to a target retention of 2.4 kg m^{-3}, which is the retention suggested for above ground use [45]. Samples were treated by submerging the dowels in a solution of 6.9% concentration and pulling a vacuum for 28 minutes followed by pressurizing the cylinder for 20 minutes. The calculated retention based off the mass uptake of 10 samples was 1.6 kg m^{-3} ± 0.3 kg m^{-3} (standard deviation).

Two types of fasteners were examined: plain carbon steel fasteners and hot-dip galvanized steel fasteners. Both fasteners were 38 mm long and approximately 3 mm in diameter (size “4d”). Prior to testing, the nails were degreased and cleaned with a 70% ethanol solution and wiped with a paper towel. The nails were then weighed to the nearest 0.1 mg and driven into pre-drilled holes (1.25 mm diameter) in the dowels. Nails were driven along the end grain (Fig. 1).

2.2. Methods

2.2.1. Isothermal calorimeter experiments

The dowels were exposed to an environment at 27°C (80°F) and near 100% relative humidity conditions; the conditions fluctuated during the 1-year exposure (see *Results*). The near 100% relative humidity conditions were obtained by placing the dowels above an aerated water bath in a temperature-controlled room. These conditions are an informal standard for corrosion measurements of metals in treated wood; data have been collected under these conditions for many wood preservatives as well as acetylated and thermally modified wood [30,46-48]. Eight samples were examined by calorimetry in this experiment; four

Fig. 1. Galvanized steel (left) and carbon steel (right) fasteners in the treated wood dowels tested in the isothermal calorimeter.

replicates with carbon steel fasteners and four replicates with hot hot-dip galvanized fasteners.

To measure the thermal power released by the corrosion reaction, the dowels were removed from the 100% relative humidity environment and placed in scintillation vials that fit in the isothermal microcalorimeter (I-Cal Flex, Calmetrix, Needham, MA) at 27°C. Steel discs with a heat capacity of approximately 10.4 J K^{-1} were used as a reference on each calorimeter cell. The vials were placed in calorimeter for 48-72 hours at a time before the samples were removed from the scintillation vials and returned to the 100% relative humidity environment. To maintain a constant wood moisture content during the experiment, the vials were tightly sealed. Vials were weighed before and after the calorimeter experiment to check for evaporation of water from the wood. In most cases the amount of evaporation was less than 0.5 mg. While tightly sealing the vials may potentially limit oxygen availability and affect the corrosion reaction, it was necessary to avoid any heat flow from water evaporation, and we were able to demonstrate that oxygen availability was not rate limiting (see *Results*).

2.2.2. Gravimetric corrosion tests

In parallel with the isothermal calorimeter experiments, gravimetric corrosion tests were also run. These tests were conducted with the same fasteners and dowels as described previously for the isothermal microcalorimetry tests (Fig. 1). Twelve replicates were tested for both carbon steel and hot-dip galvanized fasteners. Samples were removed after 2209 hours (3 months), 4368 hours (6 months), and either 9575 or 10034 hours (referred to as 1-year).

After exposure, the fasteners were removed by splitting the dowels to release the fasteners. Fasteners were then cleaned with a proprietary chelating agent (EvapoRust™, Orison Marketing, Abilene TX) diluted in a 50:50 volume ratio with water. The same cleaning procedure was used on both types of fasteners. The extra mass loss caused by the cleaning process, m_c, was tested by placing uncorroded fasteners in the same solution and measuring the mass loss. The corrosion rate, in μm yr^{-1} was then calculated by $R = K\frac{m_i - m_f + m_c}{A\rho(t_f - t_i)}$ where m is the mass (g), A is the surface area of the fastener (cm^2), ρ is the density (g cm^{-3}), t is the time (h), and K is a constant used for unit analysis (product of 8760 h yr^{-1} and 10^4 μm cm^{-1}).

After slightly longer than 1 year of exposure (10034 hours), the fasteners tested in the isothermal calorimeter were also removed from the wood and the corrosion rates were calculated gravimetrically. In doing so, we were able to compare the total amount of corrosion the fasteners exhibited against the total amount of heat released from the samples for eight individual samples (four replicates of each fastener type).

3. Results and discussion

3.1. Determination of thermal power

Fig. 2 shows data from a representative microcalorimetry measurement. The first 12 hours of the data (labeled "a" in Fig. 2) contained a large swing in the thermal power as the samples came to thermal equilibrium in the microcalorimeter and was excluded. Once this initial disruption had resolved, the samples exhibited a constant thermal power ("b" in Fig. 2). At 47 hours, the samples were removed from the calorimeter. Data collection continued for several more days to obtain an appropriate baseline ("c" in Fig. 2).

In all experiments, the data exhibited small fluctuations around a constant value. This behavior is consistent with uniform corrosion where there is no preferential corrosion sites and small areas on the surface alternate between being the cathode and anode in the corrosion reaction. Based upon electrochemical noise and isothermal calorimetry measurements, we would expect non-uniform corrosion, such as pitting or crevice corrosion, to appear as large spikes in the thermal power during pit nucleation followed by an exponential decay [49,50]. The uniform corrosion observed in this experiment agrees with previous observations of metals embedded in treated wood [47].

3.2. Effect of oxygen on the reaction

Oxygen is typically consumed as part of the cathodic corrosion reaction. Since the vials were tightly sealed during the experiment, it is possible that the partial pressure of oxygen may have decreased during the calorimeter experiment.

While most data appeared similar to the data in Fig. 2 where the thermal power was nearly constant with time, there were several measurements that appeared much different. These anomalous data can help us understand the importance of sealing the vials and whether the oxygen limited the reaction rate in the majority of the experiments.

In early measurements, vials were not completely sealed but instead lids were loosely placed on the vials. In these experiments, the wood in the unsealed vials lost an average of 0.20 g of moisture, which resulted in a moisture content reduction of 4.5% MC. The results of these experiments can be seen in Fig. 3a. These data exhibit a strong endothermic heat flow (1-2 mW) from the evaporation of water from the

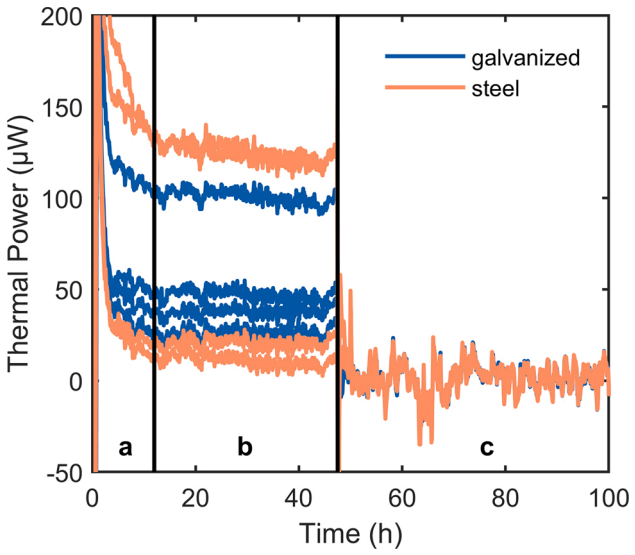

Fig. 2. Representative data collected during the first month of the 1-year exposure. The samples were placed in the calorimeter at t=0, reached thermal equilibrium (a), exhibited a nearly constant thermal power (b), were removed and the baseline measured (c).

wood samples. This heat flow is as much as 100 times the thermal power of the corrosion reaction. Therefore, it is not possible to observe the corrosion reaction if water evaporation occurs.

On the other hand, it is possible that the sealed vials limit the total amount of oxygen in the vial and therefore limit the corrosion reaction. However, the nearly constant heat flow suggests that the reaction was not appreciably oxygen limited. In a few cases, the reaction maintained a constant heat flux for about 10 hours before decreasing (Fig. 3b). This was most commonly observed in cases where the thermal power was very high (and therefore a lot of corrosion occurred during the calorimetry experiment). The behavior in Fig. 3b is consistent with a reaction whose reagents are being consumed. In these cases, the thermal power of the corrosion reaction was taken from constant region before the decrease occurred (for example from 10-18 hours in Fig. 3b).

The data in Fig. 3 shows that to accurately measure the corrosion of metals in contact with treated wood in an isothermal calorimeter they must be placed in sealed vials (volume ~ 21 mL) to prevent evaporation. Furthermore, there appears to be enough oxygen in the vials that in most cases the corrosion reaction is not limited by the lack of oxygen.

3.3. Measured thermal powers during 1 year of exposure

The measured thermal powers for the one-year exposure test of the steel fasteners are shown in Fig. 4. Fig. 5 contains similar data for the galvanized steel fasteners. The thermal powers were determined from 24-72 h periods in the calorimeter with a constant heat flow (segment b in Fig. 2). The heats were determined from a trapezoidal integration from the measured thermal powers and the time between measurements. The average thermal powers ranged between 30-50 μW for both steel and galvanized fasteners; this signal is more than an order of magnitude above the instrument's listed precision. The resulting reaction heats during the 1-year exposure ranged from 1.0 to 1.6 kJ.

The thermal power data in Fig. 4 and Fig. 5 contain several peaks during the exposure period. The peaks occur at similar times across all samples. These peaks are a result of increases in the wood moisture content, which will be further discussed in the next section. Since the water-saturated air environment was created by storing the samples above a reservoir of water the samples occasionally were splashed with the liquid water. While unintentional, these moisture spikes (most notably near 5000 h) allowed us to gain additional insights into the effect of moisture on the corrosion reaction by giving us additional data on the moisture content dependence of the corrosion rate (Fig. 6).

3.4. Effect of moisture on the corrosion reaction

While the time series of thermal power measurements (Fig. 4 and Fig. 5) is necessary for calculating the heat of the reaction for comparison against the gravimetric corrosion rate, the measured thermal powers can also be plotted as a function of wood moisture content, as shown in Fig. 6.

The data in Fig. 6 are consistent with previous data on the moisture dependence of the corrosion rate of metals embedded in treated wood. The enthalpy is nearly zero until 15% moisture content, at which point the enthalpy climbs with moisture content. However, unlike the previous electrochemical measurements, the data appear to have a more gradual increase in the rate of corrosion with moisture content. The electrochemical measurements are highly affected by the electrical resistance of the wood, which itself is a strong function of moisture content [51]. As a result, the electrochemical measurements may underpredict the amount of corrosion at low moisture content. While understanding the relationship between the corrosion rate and the moisture content is extremely important for the practical use of fasteners in treated wood, the limited data that existed was strongly influenced by these measurement difficulties.

It appears that isothermal calorimetry may be a more direct way to measure the moisture dependence of the corrosion rate. The measurement of the thermal power does not depend upon the electrical resistance or other sample properties. Additionally, the variation in the moisture content throughout the experiment produced a wide range of measured enthalpies and moisture content. While there is a high amount of scatter in Fig. 6, these experimental data are a result of the moisture content fluctuating away from a target moisture content. The measured moisture contents (on the x-axis of Fig. 6) are the average moisture content of the dowel; there were almost certainly moisture gradients within the samples and the exact moisture content around the fastener is uncharacterized. The data in Fig. 6 suggest that isothermal calorimetry may be a useful tool for evaluating the moisture dependence of the corrosion reaction if the moisture content of the samples were more carefully controlled.

3.5. Gravimetric corrosion rates

The gravimetric data collected in the experiment are given in Fig. 7. The boxplots are based on 12 replicates at 3 and 6 months of exposure and 24 replicates at the final measurement time of 1 year. The corrosion

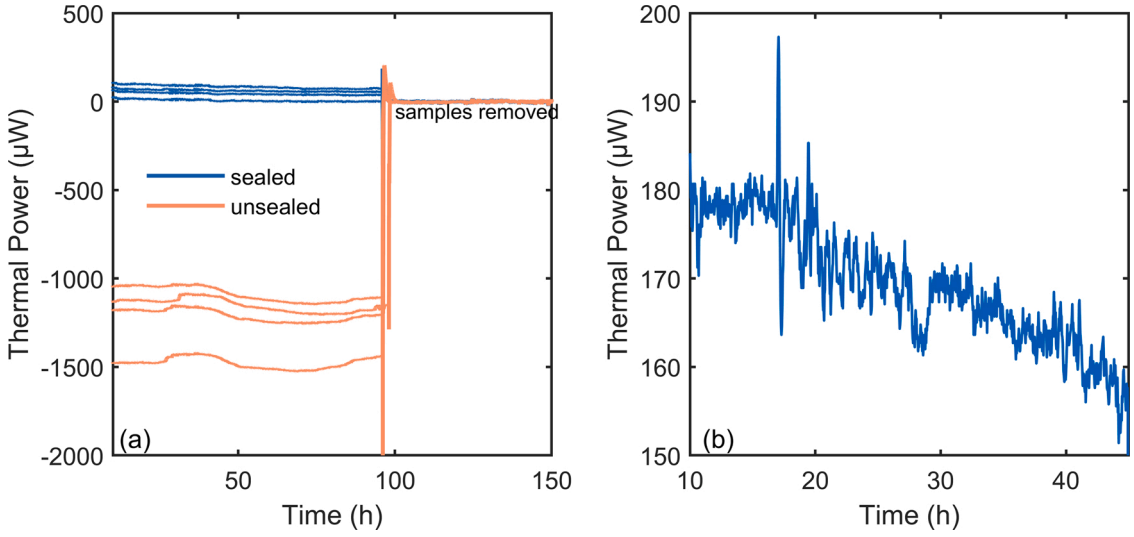

Fig. 3. (a) Example showing unsealed vials that exhibited evaporation during the measurement. (b) Example with a high corrosion rate where the oxygen was consumed and the thermal power decreased at long times. The first 10 hours of data were discarded from the large spike in thermal power due to thermal equilibration

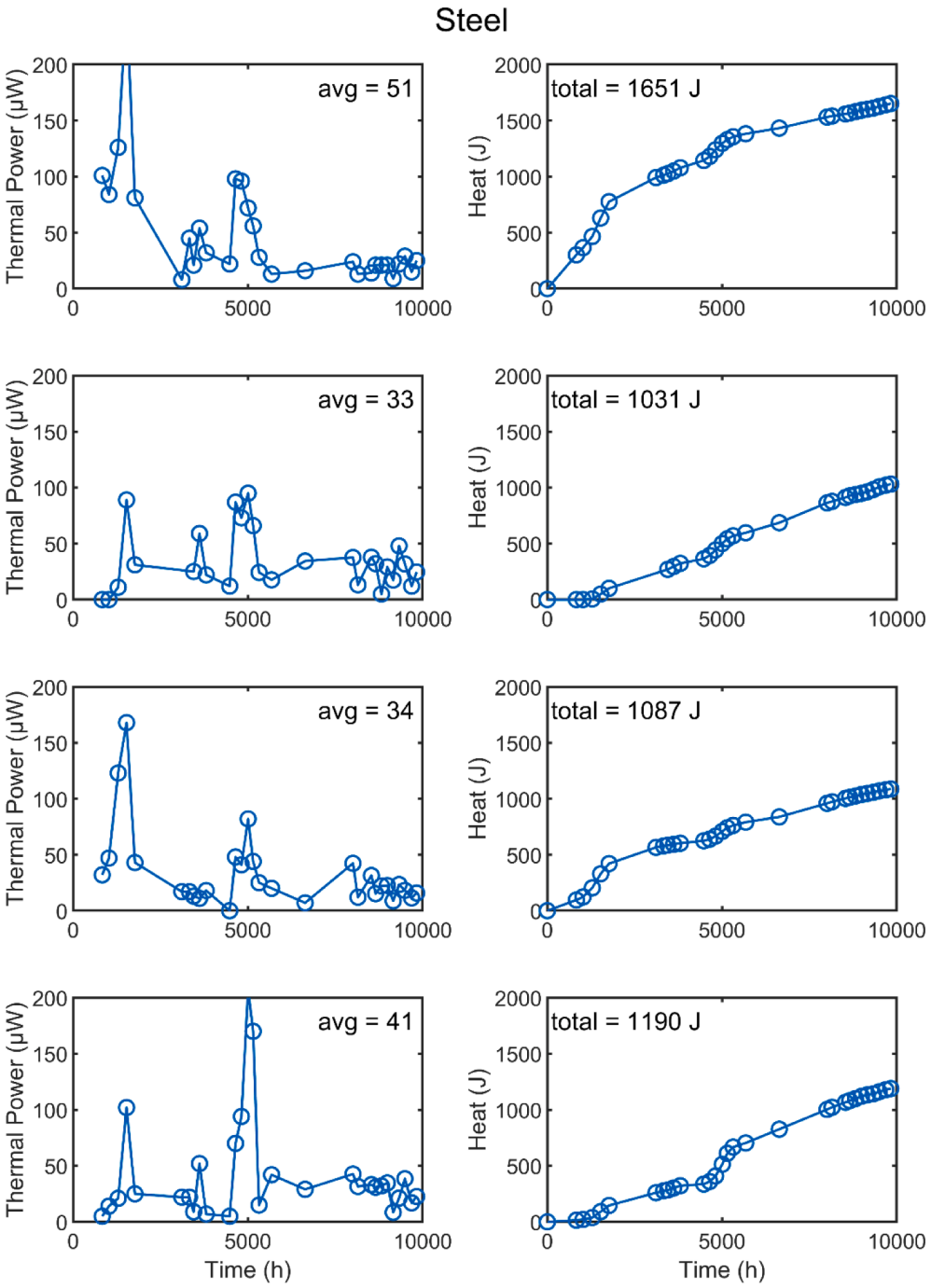

Fig. 4. Thermal powers (left column) and heat (right column) of the four replicates of the steel fasteners.

rates measured at 3 months show the highest corrosion rate and this was observed for both the galvanized and steel specimens. A Tukey HSD test revealed the corrosion rate at 3 months was statistically significantly higher than the rate at 6 months and 1 year ($p = 0.05$). Corrosion rates at 6 months and 1 year were not significantly different ($p = 0.05$).

Outside of this study, limited data exists on whether the corrosion rate of metals embedded in wood decreases with exposure time immediately after exposure. Zelinka and Rammer [30] removed 3 replicates monthly over the first 3 months of exposure and quarterly for the remainder of a 1-year exposure test. They found that the corrosion rates measured within the first 3 months were on average higher than those measured at 6, 9, and 12 months; however the results were not statistically significant and the uncertainties in the measurements were much greater at these shorter times because the mass losses were small [52].

The current measurements exhibit statistically higher corrosion rates at times shortly after exposure. However, it is unclear whether this is a result of a passivation reaction that inhibits further corrosion or is a result of moisture fluctuations in the sample. For example, the data in Fig. 6 show that the corrosion rate is strongly dependent on the wood moisture content regardless of when the measurement was taken. Further insight can be seen in the far right panel of Fig. 7 which plots the moisture content measurements collected over these three time periods on the 8 samples placed in the calorimeter. Each boxplot contains all of the moisture contents measured over the time period; therefore the 1-year boxplot contains all of the 3 and 6 month data within it, and the 6 month boxplot contains all of moisture content measurements collected within the first 3 months. The moisture boxplots exhibit the same behavior as the corrosion rate data; the moisture contents

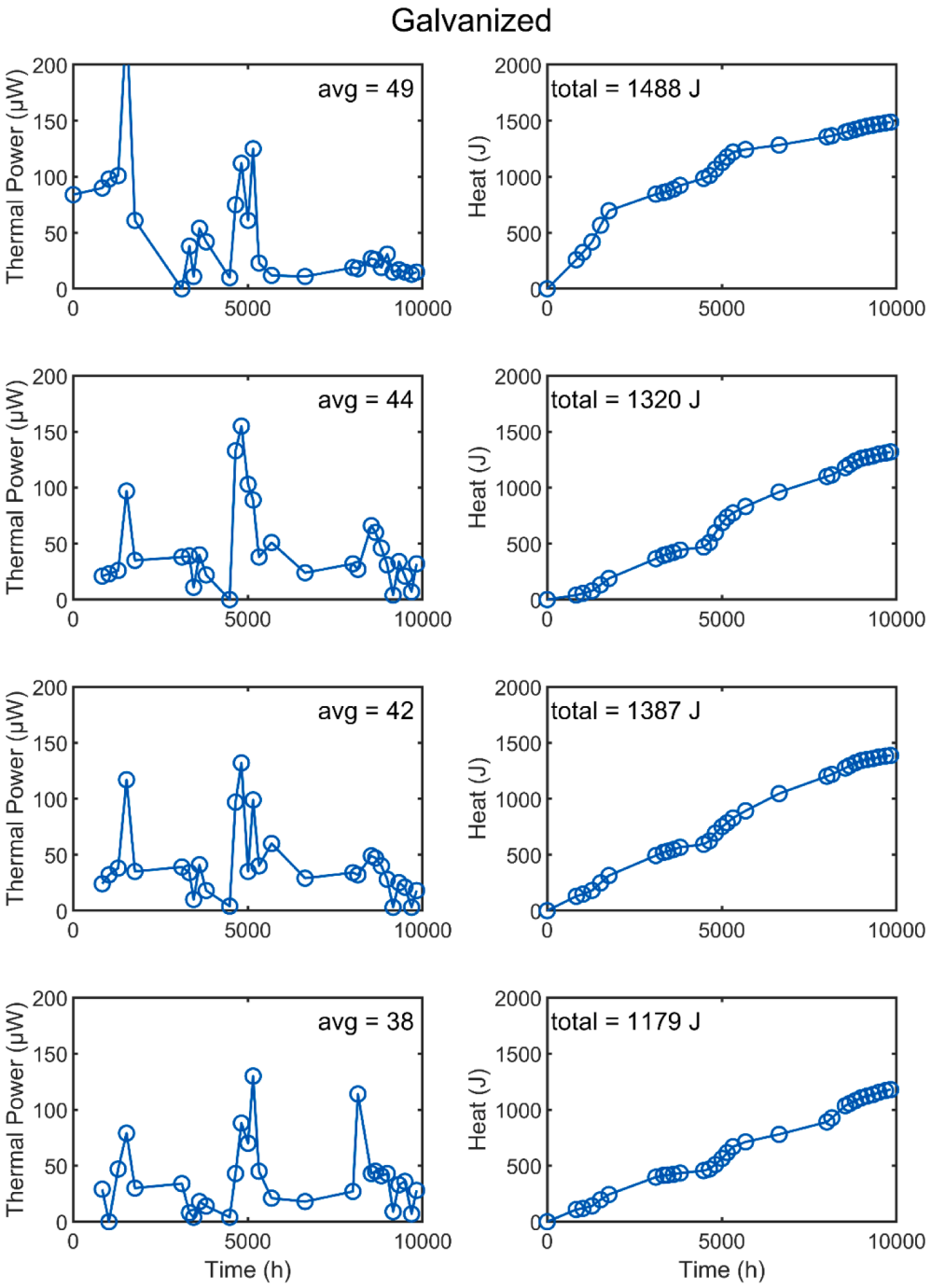

Fig. 5. Thermal powers (left column) and heat (right column) of the four replicates of the galvanized steel fasteners.

measured at 3 months were statistically significantly higher than those measured at 6 months and 1 year. In summary, there are two possible explanations for the higher corrosion rates measured in the first 3 months. The corrosion rate may decline over time because of passivation or because of decreasing moisture content. These data are consistent with the data of Zelinka and Rammer [30] and highlight the need for more data on how the corrosion reaction proceeds within the first weeks and months after exposure.

3.6. Comparison of the mass loss and the measured reaction enthalpies

The data in Fig. 6 and Fig. 7 suggest that the thermal power data collected using isothermal calorimetry can capture the kinetics of the corrosion reaction. However, while the thermal powers are proportional to the corrosion reaction, the corrosion rate is what is needed for wood engineering applications.

The reaction enthalpy is needed to calculate the corrosion rate from the thermal power; the mass loss Δm (g) can be expressed by

$$\Delta m = \frac{Q \cdot M}{\Delta_r H}$$

where $\Delta_r H$ is the enthalpy of the reaction (J mol^{-1}), M is the molar mass (g mol^{-1}) of the metal, and Q is the heat (J) measured over the exposure period.

A comparison of the mass loss and the heat after 1 year of exposure is

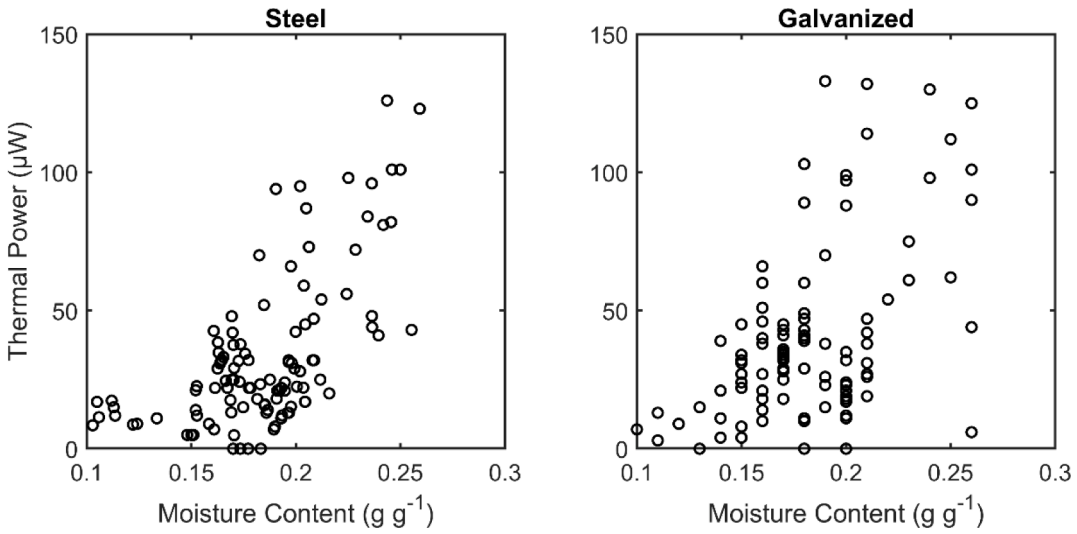

Fig. 6. Measured thermal powers as a function of wood moisture content during a 1-year exposure in treated wood.

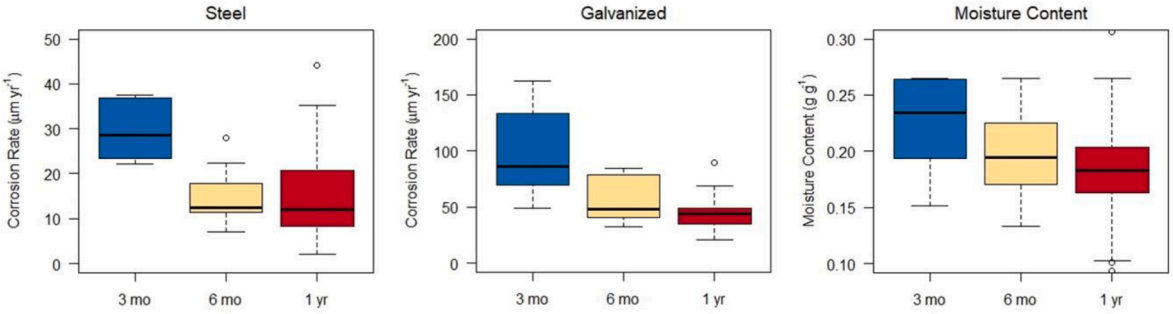

Fig. 7. Gravimetric corrosion rates taken after 3 month, 6 months, and 1 year of exposure in ACQ-D treated pine. The moisture contents measured during these time periods are given in the far right column.

presented in Fig. 8 (circles). Reaction enthalpies were calculated from tabulated enthalpy of formation data and Hess's law (see Appendix). Previous studies of the corrosion products for metals embedded in treated wood have identified several different potential corrosion products [47]. Therefore, the theoretical heats from these reactions are plotted in Fig. 8 as a shaded region rather than a straight line. Because the determination of the gravimetric corrosion rate is a destructive process, there are only eight data points where both the reaction heat

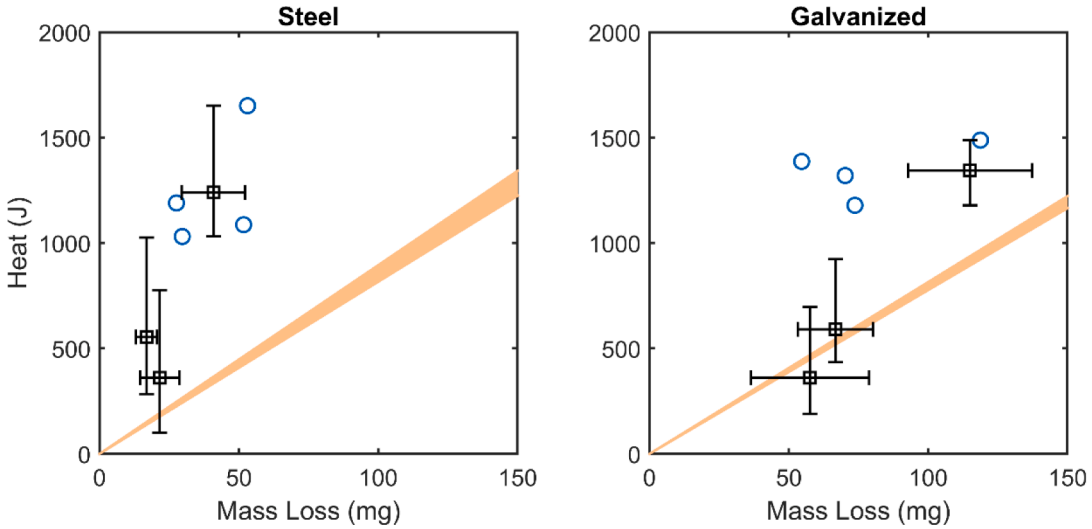

Fig. 8. Measured heats plotted as a function of the mass losses. The circles represent individual replicates at 1-year of exposure. The squares represent the mean of the 12 replicates (mass loss) and the 4 calorimeter replicates (heat). Error bars are the 95% confidence interval of the mass loss and the maximum and minimum heat measured. The shaded region represents range of predicted heats for a given mass loss based upon tabulated enthalpies of reaction.

and mass loss were known. However, additional insights can be gained by comparing the average heat against the mass losses measured at 3 and 6 months of exposure. These data are presented as squares with error bars describing the range of measured mass losses and heats.

For the galvanized steel data, the experimental data at 3 and 6 months of exposure lie very close to the theoretical calculations. However, the data at 12 months lie above predicted enthalpies for the reaction. For the steel data, all measured values were greater than predicted from the enthalpies calculated from Hess's law. It could be that the enthalpies of reactions used in the calculations do not accurately represent the complex corrosion reaction of metals in contact with treated wood where metal ions often form organometallic compounds with wood polymers. Another possibility is that there is an additional exothermic chemical or biological reaction occurring during the experiment whose enthalpy was contributing to part of the measured heat. One obvious potential source of an exothermic reaction is the breakdown of wood by decay or mold fungi. ACQ treated wood is already resistant to wood decay fungi, which use enzymes and other chemicals to break down the structural polymers of wood. However, certain types of mold fungi can grow on ACQ treated wood. In fact, observations of the wood plugs following the experiment with a stereomicroscope showed evidence of mold growth on at least some of the samples. Mold growth during the experiment may have increased the evaluated heat. However, the amount of mold growth during the time the samples were in the calorimeter is unknown and the data cannot be adjusted or corrected for this.

Since most moldicides do not affect the corrosion of metals in wood [53], future experiments should be conducted on wood treated with moldicide in addition to the wood preservative of interest.

4. Conclusions

Isothermal calorimetry measurements were collected on metals embedded in ACQ-treated wood throughout a 1-year exposure period. The following conclusions can be drawn from the measurements:

- The results further confirm that the primary corrosion mechanism is uniform corrosion for embedded fasteners in ACQ-treated wood.
- Isothermal calorimetry appears to be a promising method for determining how the corrosion rate depends upon the wood moisture content. The measured thermal powers depended upon the wood moisture content and the technique has a high enough resolution to measure small changes in the corrosion rate. Unlike electrochemical measurements, isothermal calorimetry does not have systematic errors that depend upon the moisture content.
- Gravimetric corrosion rates showed higher corrosion rates at 3 months of exposure than those measured after 6 and 12 months. However, the moisture content during the first 3 months of exposure was also higher than 6 and 12 months. More work (with a constant moisture content) is needed to determine whether factors other than moisture content cause the corrosion rate to change with time.
- The measured heats were proportional to the measured mass loss data. However, the enthalpies evaluated from heat and mass loss data were greater than the standard reaction enthalpies. Further work should investigate whether mold growth on the samples affected the measurements.
- More work is needed to better understand why the measured enthalpies were in some cases greater than the standard reaction enthalpy.

Declaration of Competing Interest

The authors declare that they have no known competing financial interests or personal relationships that could have appeared to influence the work reported in this paper.

Data availability

Data will be made available on request.

Acknowledgements

The authors thank Forest Products Laboratory colleagues Steve Halverson for treating the samples with ACQ and Rachel Arango for help with the moldicide treatments of the wood samples. This paper was improved by many conversations with Lars Wadsö of Lund University on the topic of isothermal calorimetry.

Appendix: Reaction enthalpy calculations

The observed iron corrosion products were goethite (α-FeOOH) and magnetite (Fe_3O_4), while the observed zinc corrosion products were namuwite [$Zn_4(SO_4)(OH)_6{\cdot}4H_2O$], hydrozincite [$Zn_5(CO_3)_2(OH)_6$], smithsonite ($ZnCO_3$), and zincite, (ZnO) (Zelinka et al. 2010).

The observation of multiple reaction products for each metal implies that several oxidation reactions occur simultaneously. Here we estimate the enthalpies of the likely reactions and identify maximum and minimum values for each metal to give the shaded regions in Fig. 8.

Standard enthalpies of formation for relevant chemical substances are summarized in Table A1. No value for namuwite could be found in the literature. The likely oxidation reactions are listed in Table A2, along with the enthalpies calculated using Hess's Law and the values in Table A1. These reactions assume aqueous Cu^{2+} rather than absorbed Cu^{2+} in wood; the enthalpy of sorption is accounted for below.

The enthalpy of sorption of aqueous Cu^{2+} in milled pine wood was estimated to be +17.8 kJ mol^{-1} by Semerjian (2018). Using this value, along with the range of standard reaction enthalpies in Table A2, the range of reaction enthalpies for oxidation of iron and zinc in wood containing Cu^{2+} are as follows:

Fe oxidation: –500 kJ $mol^{-1} \leq \Delta_r H \leq$ –456 kJ mol^{-1}

Zn oxidation: –508 kJ $mol^{-1} \leq \Delta_r H \leq$ –433 kJ mol^{-1}

These ranges are indicated as shaded regions in Fig. 8.

References

Chase, M.W. 1998. NIST-JANAF Thermochemical Tables, 4th Edition, American Institute of Physics, https://janaf.nist.gov/

Cox, J.D., Wagman, D.D., and Medvedev, V.A. 1989. CODATA Key Values for Thermodynamics. Hemisphere Publishing Corp., New York. http://codata.info/resources/databases/key1.html

Table A1
Standard enthalpy of formation ($\Delta_f H^\circ$) for substances at 298.15 K

Substance	$\Delta_f H^\circ$ (kJ mol^{-1})
CO_2(g)	–393.522[a]
Cu^{2+}(aq)	+64.9[b]
α-FeOOH(s) (goethite)	–560[c]
Fe_3O_4(s) (magnetite)	–1120.894[a]
H_2O(l)	–285.830[a]
$ZnCO_3$ (smithsonite)	–818.9[d]
$Zn_5(CO_3)_2(OH)_6$(s) (hydrozincite)	–3584[d]
ZnO(s) (zincite)	–350.46[b]

[a] Chase (1998);
[b] Cox et al. (1989);
[c] Majzlan et al. (2003);
[d] Preis and Gamsjäger (2001)

Table A2
Oxidation reactions for iron and zinc, and standard reaction enthalpy $\Delta_r H^\circ$ (expressed per mole of Fe or Zn reactant)

Reaction	$\Delta_r H^\circ$ (kJ mol^{-1})
Fe(s) + Cu^{2+}(aq) + ½ H_2O(l) + ¾ O_2(g) → α-FeOOH(s) + Cu(s)	–482
Fe(s) + Cu^{2+}(aq) + 2/3 O_2(g) → 1/3 Fe_3O_4(s) + Cu(s)	–439
Zn(s) + Cu^{2+}(aq) + CO_2(g) + ½ O_2(g) → $ZnCO_3$(s) + Cu(s)	–490
Zn(s) + Cu^{2+}(aq) + 2/5 CO_2(g) + ½ O_2(g) + 3/5 H_2O(l) → 1/5 $Zn_5(CO_3)_2(OH)_6$(s) + Cu(s)	–453
Zn(s) + Cu^{2+}(aq) + ½ O_2(g) → ZnO(s) + Cu(s)	–415

Majzlan, J., Grevel, K.-D., and Navrotsky, A. 2003. Thermodynamics of Fe oxides: Part II. Enthalpies of formation and relative stability of goethite (α-FeOOH), lepidocrocite (γ-FeOOH), and maghemite (γ-Fe2O3). American Mineralogist 88(5–6): 855–859. https://doi.org/10.2138/am-2003-5-614

Preis, W., and Gamsjäger, H. 2001. Thermodynamic investigation of phase equilibria in metal carbonate–water–carbon dioxide systems. Monatshefte fuer Chemie 132: 1327–1346. https://doi.org/10.1007/s007060170020

Semerjian, L. 2018. Removal of heavy metals (Cu, Pb) from aqueous solutions using pine (*Pinus halepensis*) sawdust: Equilibrium, kinetic, and thermodynamic studies. Environmental Technology & Innovation 12: 91–103. https://doi.org/10.1016/j.eti.2018.08.005

Zelinka, S.L., Sichel, R.J., and Stone, D.S. 2010. Exposure testing of fasteners in preservative treated wood: Gravimetric corrosion rates and corrosion product analyses. Corrosion Science 52(12): 3943–3948. https://doi.org/10.1016/j.corsci.2010.08.014

References

[1] A.J. Baker, Corrosion of nails in CCA- and ACA-treated wood in two environments, Forest Prod. J. 42 (1992) 39–41.
[2] Anon, ASTM B117-03: Standard practice for operating salt spray (fog) apparatus, American Society for Testing and Materials, West Conshohocken, PA, 2005.
[3] X.G. Zhang, Corrosion of Zinc and Zinc Alloys, in: S.D. Cramer, B.S. Covino (Eds.), ASM Handbok Volume 13B, Corrosion:Materials, ASM International, Materials Park, OH, 2003, pp. 402–417.
[4] Zhang, X.G.; Hwang, J.; Wu, W.K. Corrosion testing of steel and zinc. In Proceedings of Proceedings of the 4th International Conference on Zinc and Zinc Alloy Coated Steel Sheet (GALVATECH '98), Chiba, Japan.
[5] Anon, ASTM G154-23. Standard Practice for Operating Fluorescent Ultraviolet (UV) Lamp Apparatus for Exposure of Materials, American Society for Testing and Materials, West Conshohocken, PA, 2023.
[6] Y. Wan, E.N. Macha, R.G. Kelly, Modification of ASTM B117 Salt Spray Corrosion Test and Its Correlation to Field Measurements of Silver Corrosion, Corrosion 68 (2012) I1–I10.
[7] F. Deflorian, S. Rossi, M. Fedel, Organic coatings degradation: Comparison between natural and artificial weathering, Corros. Sci. 50 (2008) 2360–2366.
[8] F. Deflorian, S. Rossi, L. Fedrizzi, C. Zanella, Comparison of organic coating accelerated tests and natural weathering considering meteorological data, Prog. Org. Coat. 59 (2007) 244–250, https://doi.org/10.1016/j.porgcoat.2006.09.036.
[9] G. Bierwagen, D. Tallman, J. Li, L. He, C. Jeffcoate, EIS studies of coated metals in accelerated exposure, Prog. Org. Coat. 46 (2003) 149–158, https://doi.org/10.1016/S0300-9440(02)00222-9.
[10] D.A. Jones, Principles and Prevention of Corrosion, Prentice Hall, Upper Saddle River, NJ, 1996.
[11] S.L. Zelinka, D.R. Rammer, Review of test methods used to determine the corrosion rate of metals in contact with treated wood. Gen. Tech. Rp. FPL-GTR-156, U.S. Department of Agriculture, Forest Service, Forest Products Laboratory, 2005, p. 23, p-23 p.
[12] Heim, A.L.; Davidson, G.M.; Joyce, A.R. Report of sub-committee 4 - corrosion of fastenings. New Orleans, LA; pp. 373-379.
[13] S.G. Clarke, E.E. Longhurst, The corrosion of metals by acid vapours from wood, J. Appl. Chem. 11 (1961) 435–443.
[14] D.F. Packman, The acidity of wood, Holzforschung 14 (1960) 178–183.
[15] A.J. Baker, Corrosion of metals in preservative-treated wood, in: M. Hamel (Ed.), Wood Protection Techniques and the Use of Treated Wood in Construction, Forest Products Society, Madison, Wisconsin, 1988, pp. 99–101.
[16] A.J. Baker, Corrosion of metal in wood products. Durability of Building Materials and Components. ASTM STP 691, American Society for Testing and Materials, West Conshohocken, PA, 1980, pp. 981–993.
[17] Anon, AWPA E-12: Standard method of determining corrosion of metal in contact with treated wood, American Wood Preservers' Association, Selma, AL, 2007.
[18] Anon, ASTM G198 - 11: Standard Test Method for Determining the Relative Corrosion Performance of Driven Fasteners in Contact with Treated Wood, ASTM International, West Conshohocken, PA, 2011.
[19] Jin, L.; Preston, A. Evaluation of the corrosivity of the treated wood. Laboratory vs field test methodologies. Kona, Hawaii.
[20] S.L. Zelinka, D.R. Rammer, The Use of Electrochemical Impedance Spectroscopy (EIS) to Measure The Corrosion of Metals in Contact With Wood, TMS Letters 2 (2005) 15–16.
[21] S.L. Zelinka, D.R. Rammer, D.S. Stone, Impedance spectroscopy and circuit modeling of Southern pine above 20% moisture content, Holzforschung 62 (2008) 737–744.
[22] S.L. Zelinka, D.S. Stone, D.R. Rammer, Equivalent circuit modeling of wood at 12% moisture content, Wood Fiber Sci. 39 (2007) 556–565.
[23] S.L. Zelinka, D.S. Stone, Corrosion of metals in wood: Comparing the results of a rapid test method with long-term exposure tests across six wood treatments, Corros. Sci. 53 (2011) 1708–1714, https://doi.org/10.1016/j.corsci.2011.01.039, doi:DOI:.
[24] S.L. Zelinka, D.R. Rammer, D.S. Stone, Electrochemical corrosion testing of fasteners in wood extract, Corros. Sci. 50 (2008) 1251–1257.
[25] J.K. Dennis, C. Zou, N.R. Short, Corrosion behaviour of zinc and zinc alloy coated steel in preservative treated timber, Trans. Inst. Met. Finish. 75 (1995) 96–101.
[26] N.R. Short, J.K. Dennis, Corrosion resistance of zinc-alloy coated steel in construction industry environments, Trans. Inst. Met. Finish. 75 (1997) 47–52.

[27] S.L. Zelinka, D. Derome, S.V. Glass, The effect of moisture content on the corrosion of fasteners embedded in wood subjected to alkaline copper quaternary treatment, Corros. Sci. 83 (2014) 67–74.
[28] R.A. Legault, V.P Pearson, Kinetics of the Atmospheric Corrosion of Galvanized Steel, in: S.K. Coburn (Ed.), Atmospheric Factors Affecting the Corrosion of Engineering Metals, ASTM STP 646, American Society for Testing and Materials, West Conshohocken, 1978, pp. 83–96.
[29] R.A. Legault, A.G. Preban, Kinetics of the atmospheric corrosion of low-alloy steels in an industrial environment, Corrosion 31 (1975) 117–122.
[30] S.L. Zelinka, D.R. Rammer, Corrosion rates of fasteners in treated wood exposed to 100% relative humidity, ASCE J. Mater. Civil Eng. 21 (2009) 758–763.
[31] S.L. Zelinka, D.R. Rammer, Modeling the effect of nail corrosion on the lateral strength of joints, Forest Prod. J. 62 (2012) 160–166.
[32] S.L. Zelinka, D. Derome, S.V. Glass, Combining hygrothermal and corrosion models to predict corrosion of metal fasteners embedded in wood, Build. Environ. 46 (2011) 2060–2068, https://doi.org/10.1016/j.buildenv.2011.04.017, doi:DOI:.
[33] A.L. Lavoisier, P.S. Laplace, Mémoir sur la chaleur, Mémoires de l'Académie royale des sciences (1784) 1780.
[34] T.A. Lodwig, W.A. Smeaton, The ice calorimeter of Lavosier and Laplace and some of its critics, Ann. Sci. 31 (1974) 1–17.
[35] I. Wadsö, Trends in isothermal microcalorimetry, Chem. Soc. Rev. 26 (1997) 79–86.
[36] I. Wadsö, Isothermal microcalorimetry in applied biology, Thermochim. Acta 394 (2002) 305–311, https://doi.org/10.1016/S0040-6031(02)00263-0.
[37] L. Wadsö, F. Gómez Galindo, Isothermal calorimetry for biological applications in food science and technology, Food Control 20 (2009) 956–961, https://doi.org/10.1016/j.foodcont.2008.11.008.
[38] J. Telegdi, H. Otmacic-Curkovic, K. Marusic, F. Al-Taher, E. Stupnisec-Lisac, E. Kálmán, Inhibition of copper corrosion by self assembled amphiphiles, Chem. Biochem. Eng. Q. 21 (2007) 77–82.
[39] J. Telegdi, T. Szabó, F. Al-Taher, É. Pfeifer, E. Kuzmann, A. Vértes, Coatings against corrosion and microbial adhesion, Mater. Corros. 61 (2010) 1000–1007, https://doi.org/10.1002/maco.201005797.
[40] K. Tomantschger, R. Findlay, M. Hanson, K. Kordesch, S. Srinivasan, Degradation modes of alkaline fuel cells and their components, J. Power Sources 39 (1992) 21–41, https://doi.org/10.1016/0378-7753(92)85003-S.
[41] Chin, A.; Ellison, D.S.; Farmer, H.A.; Crowley, D.R. Microcalorimetric method to determine the corrosion rate of liquid propellant and metal container. In Proceedings of Proceedings of the Workshop on the Microcalorimetry of Energetic Matierials, Leeds, United Kingdom; pp. N1-N14.
[42] D. Orlov, B. Reinwalt, I. Tayeb-Bey, L. Wadsö, J. Horky, A. Ojdanic, E. Schafler, M. Zehetbauer, Advanced immersion testing of model mg-alloys for biomedical applications. Magnesium Technology 2020, Springer, 2020, pp. 235–242.
[43] D. Singh, D.A. Basha, L. Wadsö, D. Orlov, Y. Matsushita, A. Singh, S.S. Hosmani, Evolution of gradient structured layer on AZ91D magnesium alloy and its corrosion behaviour, J. Alloys Compd. 882 (2021), 160659, https://doi.org/10.1016/j.jallcom.2021.160659.
[44] Anon, AWPA P5: Standard for waterborne preservatives, American Wood Protection Association, Birmingham, AL, 2007.
[45] Anon, AWPA Standard U1: Use Category System. User Specifications for Treated Wood, American Wood Protection Association, Birmingham, AL, 2019.
[46] S.L. Zelinka, L. Passarini, Corrosion of metal fasteners embedded in acetylated and untreated wood at different moisture contents, Wood Mater. Sci. Eng. (2018), https://doi.org/10.1080/17480272.2018.1544171. Online ahead of print.
[47] S.L. Zelinka, R.J. Sichel, D.S. Stone, Exposure testing of fasteners in preservative treated wood: gravimetric corrosion rates and corrosion product analyses, Corros. Sci. 52 (2010) 3943–3948.
[48] S.L. Zelinka, L. Passarini, F.J. Matt, G.T. Kirker, Corrosiveness of Thermally Modified Wood, Forests 11 (2020) 50.
[49] K. Sasaki, H. Isaacs, Origins of electrochemical noise during pitting corrosion of aluminum, J. Electrochem. Soc. 151 (2004) B124.
[50] J. Smulko, K. Darowicki, A. Zieliński, Pitting corrosion in steel and electrochemical noise intensity, Electrochem. Commun. 4 (2002) 388–391.
[51] S.V. Glass, S.L. Zelinka, Chapter 4. Moisture Relations and Physical Properties of Wood, in: R.J. Ross (Ed.), Wood Handbook. Wood as an Engineering Material. FPL-GTR-282, U.S. Department of Agriculture, Forest Service, Forest Products Laboratory, 2021.
[52] S.L. Zelinka, Uncertainties in corrosion rate measurements of fasteners exposed to treated wood at 100% relative humidity, ASTM J. Test. Eval. 35 (2007) 106–109.
[53] R.A. Arango, S.T. Lebow, V. Yang, S.L. Zelinka, P.K. Lebow, P. DeWald, Evaluation of moldicidal additives for wood preservatives used in dip-treatment of wood packaging materials for military applications, U.S. Department of Agriculture, Forest Service, Forest Products Laboratory, 2023, 2023/01/12.